UNIVERSITY OF BATH

University of Bath

Acceleration Decoupling Control of 6 Degree of Freedom Electro-hydraulic Shaking Table

Guang-feng Guan

Department of Mechanical Engineering, Dalian Maritime University. Dalian 116026, China. gfguan@126.com

A.R.Plummer

Centre for Power Transmission and Motion Control, Department of Mechanical Engineering, University of Bath. Bath BA2 7AY, UK. A.R.Plummer@bath.ac.uk

Abstract: Electro-hydraulic shaking tables are widely used for vibration testing where high force and displacement amplitudes are required. In particular, they are a vital tool in seismic testing, enabling the development of buildings and other structures which are earthquake resistant. Three-variable-control (TVC) is commonly used for the control of multi-degree of freedom (DOF) electro-hydraulic shaking tables. However the coupling between the degrees of freedom is often significant and is not compensated by TVC. In this paper, an acceleration decoupling control (ADC) method is presented for a 6 DOF electro-hydraulic shaking table system to improve the acceleration tracking performance and decouple the motion in task space. The gravitational, coriolis and centripetal forces are compensated in joint space based on a dynamic model of the shaking table. Modal control is used to transform the coupled dynamics into six independent systems. Inverse dynamics models are used to cancel the differences in actuator dynamics. The proportional gains in modal space are tuned heuristically to give sufficient stability margins to provide robustness in the presence of modeling errors. The input filter and feedforward controller in TVC are added to improve the acceleration tracking performance of each independent system. Experimental acceleration frequency responses are used to demonstrate the effectiveness of ADC, and in particular these show a consistent reduction in cross-axis coupling compared to TVC. Moreover, only 4 parameters need to be tuned, as opposed to 36 for TVC, and the method provides a viable route to improving the accuracy of seismic testing in the future.

Keywords: electro-hydraulic shaking table, TVC, modal control, acceleration control, seismic testing.

I. Introduction

Multi-degree of freedom (DOF) electro-hydraulic shaking tables can generate both large forces and large strokes and are widely used for seismic testing [1]. The accurate replication of the measured acceleration amplitude is essential to avoid significant errors in test outcomes. The ideal shaking table would be a rigid testing instrument that exactly followed the commanded motions. However, in reality there are many challenges to overcome to achieve accurate motion control, such as hydraulic and structural resonance, servo valve flow gain nonlinearity and unmodelled reaction forces exerted by the load on the table [2-5]. It is often very difficult the design a control system which fully meets the requirements of the test.

A multi-DOF electro-hydraulic shaking table is a parallel mechanism with complex nonlinearities. Motion control methods developed for parallel robots, such as the computed torque method [6, 7], inverse dynamic compensation [8] and multivariable feedback linearization [9], have been proved to be effective for Stewart platforms and similar parallel configurations. However, electro-hydraulic shaking tables need to accurately control motion at high frequencies, so the required bandwidth is much larger than that of a typical parallel robot or flight simulator motion system. Thus the application of the above-mentioned control methods is impractical, for example due to the need to handle resonances. Three-Variable-Control (TVC) is the most popular controller

structure used for electro-hydraulic shaking tables [1, 10]. Fig.1 shows a block diagram of TVC.
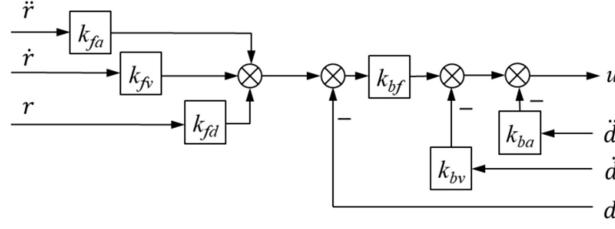

Fig.1　Block diagram of TVC

$\ddot{r}$, $\dot{r}$ and r are reference acceleration, velocity and displacement of the shaking table. $\ddot{d}$, $\dot{d}$ and d are acceleration, velocity and displacement feedback signals of the shaking table. TVC combines a feedback controller with an input filter allowing command velocity and acceleration feedforward. k_{fa}, k_{fv} and k_{fd} are feedforward gains. k_{bf}, k_{bv} and k_{ba} are feedback gains. The feedback controller includes position, velocity and acceleration terms and is used to improve the robustness and disturbance compensation performance of the system. The acceleration tracking is improved by the feedforward controller. The number of parameters for TVC is six for each DOF. In practice TVC is normally manually tuned, and so the level of shaking table performance achieved is dependent on the skill of the operator [1]. However, TVC is a single-axis control method, and so the dynamic cross-coupling among degrees of freedom is not taken into account. These limitations often mean the performance capability of a shaking table is not fully utilized to optimize the accuracy of a test. Outer loop compensation, i.e. iterative learning control, is sometimes used to correct the limitations of TVC and improve the accuracy of the test [11-14]. However, repeated iterations are often not effective nor acceptable due to damage caused to the structure during the test [5]. Hence improvements in closed-loop control have been sought.

A modal control approach for multi-DOF hydraulic mechanisms was first described in [15]. The signals in task space including the control errors, control inputs and outputs are transformed into the decoupled modal space. The control parameters of each DOF in modal space can be tuned independently and the bandwidths in task space are extended. The modal control approach has been applied to flight simulator motion systems and can improve the dynamic performance in each DOF [16-18]. Experimental results with a model-based controller which included modal control gave a 6-fold increase in bandwidth compared with a proportional controller, and the overturning sensitivity was reduced by between 5dB and 15dB [19]. An inverse actuator dynamics model was used in the controller to cancel the actuator dynamics and extend the bandwidth of the control system. However compensations for additional forces such as weight are not taken into account in [19].

Acceleration Decoupling Control (ADC) is developed in this paper to improve the control performance of 6 DOF electro-hydraulic shaking tables. Modal space control with dynamic compensation is developed based on the dynamic model of the system. The influence of the platform and load weight is taken into account in the controller, as appropriate for a shaking table without a physical weight compensation system. The load pressures and the accelerations of the hydraulic actuators are used to compensate the influence of the gravity term and the coriolis/centripetal term in joint space. An inverse actuator dynamics model is developed to cancel

the actuator dynamics differences in modal space. The same proportional gains are set for each DOF and the cross-coupling systems are decoupled into 6 independent systems with the same dynamic characteristics in task space. The input filter and feedforward controller in TVC are used to improve the acceleration tracking performance of each independent system.

This paper is organized as follows. Section 2 describes the modal space control with dynamic compensation. Section 3 presents the ADC approach for a 6 DOF electro-hydraulic shaking table. Experimental results are given in Section 4. Section 5 concludes the paper.

II. Modal space control with dynamic compensation

Fig.2 shows the structure of the 6 DOF electro-hydraulic shaking table which is used to validate the controller in this research. The major specifications of the shaking table are given in Table 1. The table is of conventional design and typical of many 6 DOF tables currently in use for seismic testing.

The control point of the 6 DOF shaking table is set to the center of the square formed by the upper gimbals of horizontal actuators. The 6 DOF are X, Y, Z, Rx, Ry and Rz respectively.

2.1 Compensation of the gravity and coriolis/centripetal forces in joint space

The dynamic model for parallel motion platform as a rigid body in the task space can be written as [9, 20]

$$J_{\text{lq}}^T f_a = M_t \ddot{q} + C_t + G_t \tag{1}$$

where M_t is the generalized inertia matrix in task space. q is the position vector of the motion platform with respect to the fixed base frame. $\ddot{q}$ is the acceleration vector of the motion platform. C_t is the coriolis/centripetal term. G_t is the gravity force vector. f_a is the actuator output force vector. J_{lq} is the Jacobian matrix of the platform that maps the actuator output forces to the forces/torques in task space.

J_{lq} also relates the platform velocities, $\dot{q}$, to the actuator velocity in joint space, $\dot{l}_a$

$$\dot{l}_a = J_{\text{lq}}\dot{q} \tag{2}$$

The limited stroke of most shaking tables means that the geometric changes are small within the working range and so J_{lq} can be considered to be constant. The relation between the acceleration vector of the actuators $\ddot{l}_a$ and $\ddot{q}$ can be approximately represented as [9, 17, 21, 22]

$$\ddot{l}_a = J_{\text{lq}}\ddot{q} \tag{3}$$

Substituting Eq. (3) into Eq. (1), we get actuator force as

$$f_a = M_a^{-1}\ddot{l}_a + F_d \tag{4}$$

where M_a is the joint space mass matrix, $M_a = J_{\text{lq}}M_t^{-1}J_{\text{lq}}^T$. The non-inertial force term is given by $F_d = \left(J_{\text{lq}}^T\right)^{-1}(C_t + G_t)$. Generally speaking, C_t is much less than G_t. In practice the variation of F_d is small when the displacement of the platform is small.
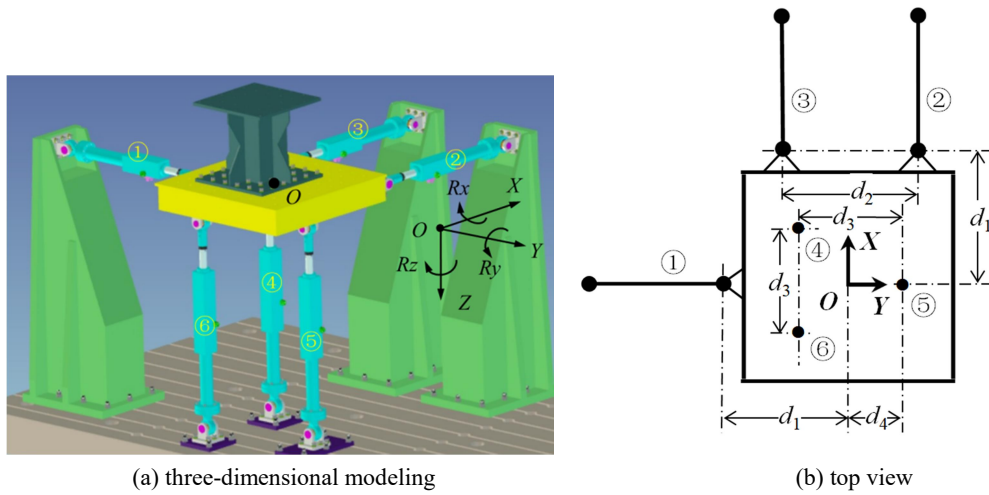
3

(a) three-dimensional modeling   (b) top view

Fig. 2   Structure of the 6 DOF shaking table in the work-ready position

Table 1. Specification of the shaking table

description	value
Size of table	1×1 m
Table mass	285 kg
Table moments of inertia	[27 27 53] kgm^2
Load mass	145kg
Load moments of inertia	[9.5 9.5 6] kgm^2
Center of gravity of the load	[-0.1 0 -0.32] m
Peak velocity–vertical	0.22 m/s
Peak acceleration–vertical	2 g
Valve rated flow	30 l/min @ 210bar
Valve natural frequency	>100 Hz
Valve damping ratio	0.7
Oil supply pressure	100 bar
Piston/rod diameter	0.063/0.045 m
Actuator stroke	0.15 m
d_1 Distance between the upper gimbal of the actuators in X/Y direction and the OY/OX axis	0.585 m
d_2 Distance between the upper gimbals of the two actuators in X direction	0.77 m
d_3 Distance between the upper gimbals of the actuators in Z direction	0.6 m
d_4 Length of the projection of the line between upper gimbal of the actuators in Z direction and the control point in OY axis	0.3 m
Distance between the upper gimbals and lower gimbals of the actuators in X/Y direction in work-ready position	1.072 m
Distance between the upper gimbal and lower gimbal of the actuators in Z direction in work-ready position	1.294
Distance between the upper gimbals plane of the actuators in X/Y direction and the upper gimbals plane of the actuators in Z direction	0.162 m

The linearised hydraulic models for a symmetrical valve and a symmetrical actuator with inertial load are given as [23]

$$x_{vi} = V(s)k_d u_{ai} \tag{5}$$

$$Q_{Li} = k_q x_{vi} - k_c p_{Li} \tag{6}$$

$$Q_{Li} = Asl_{ai} + \left(C_{tc} + \frac{V_t}{4\beta_e}s\right)p_{Li} \tag{7}$$

$$f_{ai} = Ap_{Li} \tag{8}$$

where u_{ai} is control signal of the ith valve, k_d is the electrical conversion gain. $V(s)$ is the spool dynamic response characteristic, $V(s) = \frac{1}{\frac{s^2}{\omega_v^2} + \frac{2\xi_v}{\omega_v}s + 1}$, where ξ_v and ω_v are the damping ratio and natural frequency of the valve respectively [23]. x_{vi} is spool position of the ith valve, k_q is flow rate coefficient of the valve, k_c is the ratio of flow rate reduction to load pressure of the valve, p_{Li} is load pressure of the ith hydraulic actuator, Q_{Li} is the load flow of the ith actuator, A is effective piston area of the actuator, l_{ai} is displacement of the ith actuator, C_{tc} is the leakage coefficient, V_t is the capacity of the actuator, β_e is bulk modulus of the fluid, and f_{ai} is output force of the ith actuator.

Eqs. (4)~(8) provide the main equations to describe the dynamic model of the motion platform in joint space which is shown in Fig. 3, where $k_{ce} = k_c + C_{tc}$.
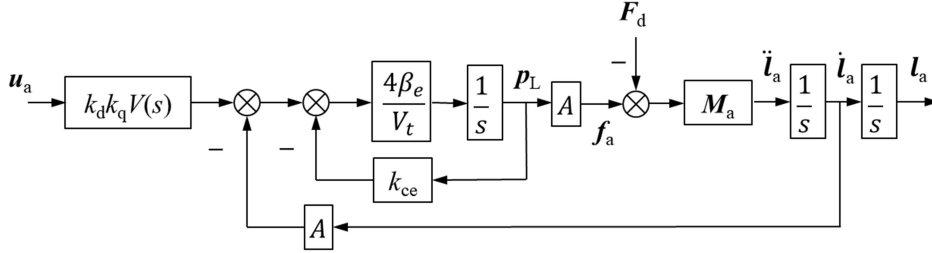

Fig. 3   Dynamic model of the motion platform in joint space

Defining $\widehat{\boldsymbol{F}}_d$ as estimate of $\boldsymbol{F}_d$. Combing Eq. (4) and (8) gives

$$\widehat{\boldsymbol{F}}_d = A\boldsymbol{p}_L - \boldsymbol{M}_a^{-1}\ddot{\boldsymbol{l}}_a \tag{9}$$

Based on Fig. 3, the gravity and coriolis/centripetal forces can be compensated [24-25]. Fig. 4 shows the compensation scheme.

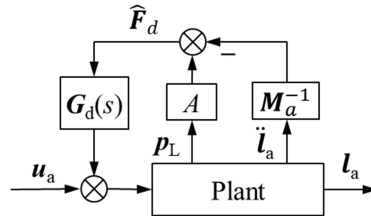Fig. 4   Block diagram of compensation of the gravity and coriolis/centripetal forces

$\boldsymbol{G}_d(s)$ in Fig.4 are given by

$$\boldsymbol{G}_d(s) = \frac{1}{Ak_d k_q}\left(k_{ce} + \frac{V_t}{4\beta_e}s\right)\boldsymbol{I} \tag{10}$$

where I is identity matrix. The valve dynamics are neglected in Eq. (10) as fast valves are typically used (in this case the valve corner frequency is about 100Hz) and the variation of F_d is small in any case.

2.2 Modal space control

Based on the compensation of the gravity and coriolis/centripetal forces, the dynamic model of the motion platform is simplified as

$$J_{lq}^T f_a = M_t \ddot{q} \tag{11}$$

Substituting the Eqs. (5)~(7) into Eq. (8), f_{ai} is given by

$$f_{ai} = \frac{A k_d k_q}{k_{ce} + \frac{V_t}{4\beta_e}s} V(s) u_{ai} - \frac{A^2}{k_{ce} + \frac{V_t}{4\beta_e}s} s l_{ai} \tag{12}$$

Assuming the dynamic characteristics of the valves and the actuators of the shaking table are the same and substituting Eq. (2) and Eq. (12) into Eq. (11), we have

$$M_t q \frac{1}{k_h}s^3 + M_t q \frac{k_{ce}}{A^2}s^2 + J_{lq}^T J_{lq} q s = J_{lq}^T u_a \frac{k_d k_q}{A} V(s) \tag{13}$$

where k_h is the stiffness of the actuator, $k_h = \frac{4\beta_e A^2}{V_t}$.

Let

$$u_a = J_{lq} P u_m \tag{14}$$
$$q = P q_m \tag{15}$$

where u_m is control signal vector of the valves in modal space. q_m is the displacement of the motion platform in modal space. P has as its columns the eigenvectors of $M_t^{-1} J_{lq}^T J_{lq}$.

Substituting Eqs. (14)~(15) into Eq. (13), we can get

$$q_m \frac{1}{k_h}s^3 + q_m \frac{k_{ce}}{A^2}s^2 + \Omega q_m s = \Omega u_m \frac{k_d k_q}{A} V(s) \tag{16}$$

where $\Omega = P^{-1} M_t^{-1} J_{lq}^T J_{lq} P = diag(\lambda_1 \quad \lambda_2 \quad ... \quad \lambda_6)$, $\lambda_1 \sim \lambda_6$ are the eigenvalues of $M_t^{-1} J_{lq}^T J_{lq}$.

Eq. (16) shows that the coupled systems in task space are converted into decoupled systems in modal space.

Let

$$u_m = G_c(s) u_m' \tag{17}$$
$$G_c(s) = \frac{A}{k_d k_q} \Omega^{-1} \left(I \frac{1}{k_h}s^2 + I \frac{k_{ce}}{A^2}s + \Omega \right)$$

Thus the open-loop transfer function between u_m' and q_m can be given by

$$q_m = \frac{V(s)}{s} u_m' \tag{18}$$

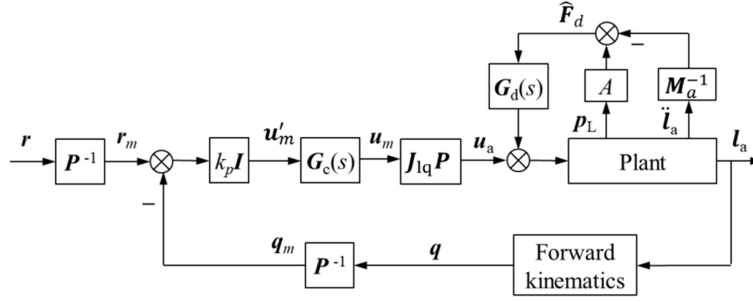Fig. 5 shows the block diagram of modal decoupling control.

Fig. 5　Block diagram of modal decoupling control

As indicated in Fig. 5, non-linear forward kinematic transformation is used to convert the displacement of the actuators from joint space to task space [9]. r is the desired displacement in task space. r_m is the desired displacement in modal space. The same proportional gain k_p is selected for each DOF in modal space in order to decouple the motion in task space. The control system is stable when k_p satisfies

$$k_p < 2\xi_v\omega_v \tag{19}$$

The shaking table motion axes are decoupled in task space and their dynamic characteristics are the same for each DOF.

III. Control structure of the ADC

The modal controller is model-based. The bandwidth could be extended greatly and the overturning sensitivity was reduced significantly if the plant model parameters are accurately determined [19]. Some of these parameters can be found from physical data, such as A, k_d and k_q. Other parameters should be estimated by experiment or experience, such as M_t, k_{ce} and k_h. There are errors in the estimation of these parameters, especially given that the model is a linear approximation. Thus it is not possible to cancel out the actuator dynamics precisely and the proportional gain, k_p, in Eq. (19) should be set small enough to ensure the stability of the control system. The small k_p limits the bandwidth of the system, but the tracking performance can be improved by including command feedforward.

The block diagram of the ADC is shown in Fig. 6. The TVC input filter is introduced to transform the acceleration command signals $\ddot{r}$ into displacement command signals and improve the tracking performance of the system by including velocity and acceleration command feedforward. Note that the 3 TVC feedback gains traditionally found within the control loop are replaced by k_pI and $G_c(s)$ in this controller, which is a second order lead term.

The parameters ω_0 and ξ_0 of the second order input filter in Fig. 6 should be set to give an approximately flat response in the required frequency range of the shaking table. k_{fa}, k_{fv} and k_{fd} are feedforward gains which are used to improve the acceleration reference tracking performance [1]. The same feedforward gains are selected for each DOF as their dynamic characteristics are similar.
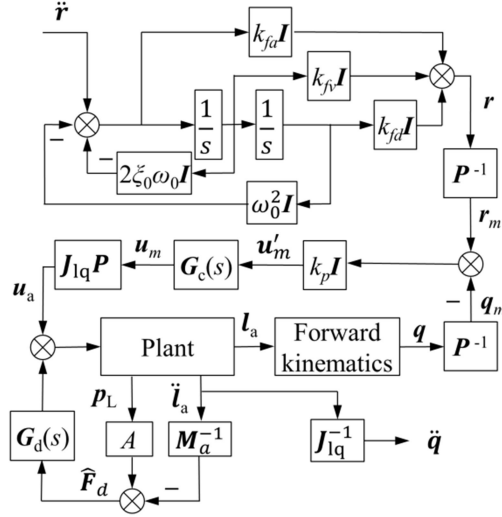
7

Fig.6   Block diagram of ADC for 6 DOF electrohydraulic shaking table

There are only 4 control parameters, k_p, k_{fa}, k_{fv} and k_{fd}, in the ADC for the 6 DOF shaking table as shown in Fig. 6.

IV. Experimental results

4.1 Experimental Setup

The experimental setup is shown in Fig. 7. Matlab/xPC Target is used as the control platform for prototyping, testing, and deploying the real-time control system for the shaking table [26, 27]. A desktop personal computer and an industrial Advantech IPC-610L are used as the host computer and the target computer respectively. The two computers communicate via a TCP/IP network. The actuators and servo-valves, which manufactured by Yantai Weihang Electrohydraulic Equipment Co., Ltd and AVIC Nanjing Servo Control System Co., Ltd respectively, are used to drive the motion platform. Temposonics magnetostrictive position sensors manufactured by MTS Sensors are used to measure the displacements of the 6 actuators. DC response accelerometers manufactured by PCB Piezotronics are used to measure the accelerations of the actuators. Gems[TM] pressure transducers are used to measure the pressures of the two chambers of the actuators. PCL 816 and PCI 1716 data acquisition cards provided the interface between the target computer and the hardware in the control loop.

4.2 Acceleration amplitude frequency response analysis

Acceleration amplitude frequency responses were measured to test the performance of the ADC. ω_0 and ξ_0 were set to be 2π and 0.7 respectively before the tests. Other controller parameters were tuned online and showed in Table 2.
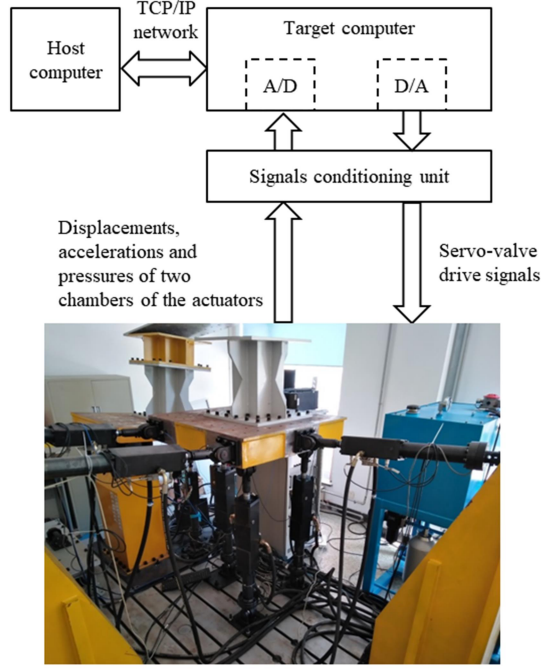
Fig. 7   Experimental setup

Table 2.   Controller parameters in the experiments

DOF		X	Y	Z	Rx	Ry	Rz
TVC	k_{fa}	4.5×10^{-4}	1×10^{-3}	1×10^{-5}	1.2×10^{-4}	2.5×10^{-4}	4.5×10^{-4}
	k_{fv}	2×10^{-2}	1×10^{-2}	5×10^{-2}	7×10^{-2}	6×10^{-2}	2×10^{-2}
	k_{fd}	1	1	1	1	1	1
	k_{bf}	1.12×10	5.5	1.12×10	1×10	8	1.12×10
	k_{bv}	1×10^{-3}	2×10^{-3}	1×10^{-3}	1×10^{-3}	1.2×10^{-3}	1×10^{-3}
	k_{ba}	1×10^{-4}	2×10^{-4}	0	0	3×10^{-5}	1×10^{-4}
ADC	k_p	1.5×10^2					
	k_{fa}	1×10^{-3}					
	k_{fv}	3×10^{-1}					
	k_{fd}	1					

Defining $\ddot{\boldsymbol{r}} = [X_{in} \quad Y_{in} \quad Z_{in} \quad Rx_{in} \quad Ry_{in} \quad Rz_{in}]$ and
$\ddot{\boldsymbol{q}} = [X_{out} \quad Y_{out} \quad Z_{out} \quad Rx_{out} \quad Ry_{out} \quad Rz_{out}]$, the acceleration frequency response function
(FRF) matrix of the closed loop 6 DOF shaking table can be expressed as

$$\begin{bmatrix} X_{out} \\ Y_{out} \\ Z_{out} \\ Rx_{out} \\ Ry_{out} \\ Rz_{out} \end{bmatrix} = \begin{bmatrix} h_{11}(\omega) & h_{12}(\omega) & \cdots & h_{16}(\omega) \\ h_{21}(\omega) & h_{22}(\omega) & & \vdots \\ \vdots & & \ddots & \\ h_{61}(\omega) & \cdots & & h_{66}(\omega) \end{bmatrix} \begin{bmatrix} X_{in} \\ Y_{in} \\ Z_{in} \\ Rx_{in} \\ Ry_{in} \\ Rz_{in} \end{bmatrix} \tag{20}$$

where $h_{11}(\omega)$ represents the FRF between X-input and X-output. h_{12} represents the FRF
between Y-input and X-output, etc. The diagonal elements of the FRF matrix are dimensionless.
The units of the non-diagonal elements of the FRF matrix are dimensionless, $(rad/s^2)/g$ or $g/(rad/s^2)$
depending on the element. The amplitude frequency response characteristics of the non-diagonal

elements of the FRF matrix represent the cross-coupling among the degrees of freedom, and need to be minimized.

The measured amplitude frequency response characteristics for $h_{11} \sim h_{66}$ with traditional TVC and the proposed new ADC are shown in Fig. 8. For the sake of brevity, only the *Ry*-related test results of the amplitude frequency response characteristics are shown in Fig. 9.
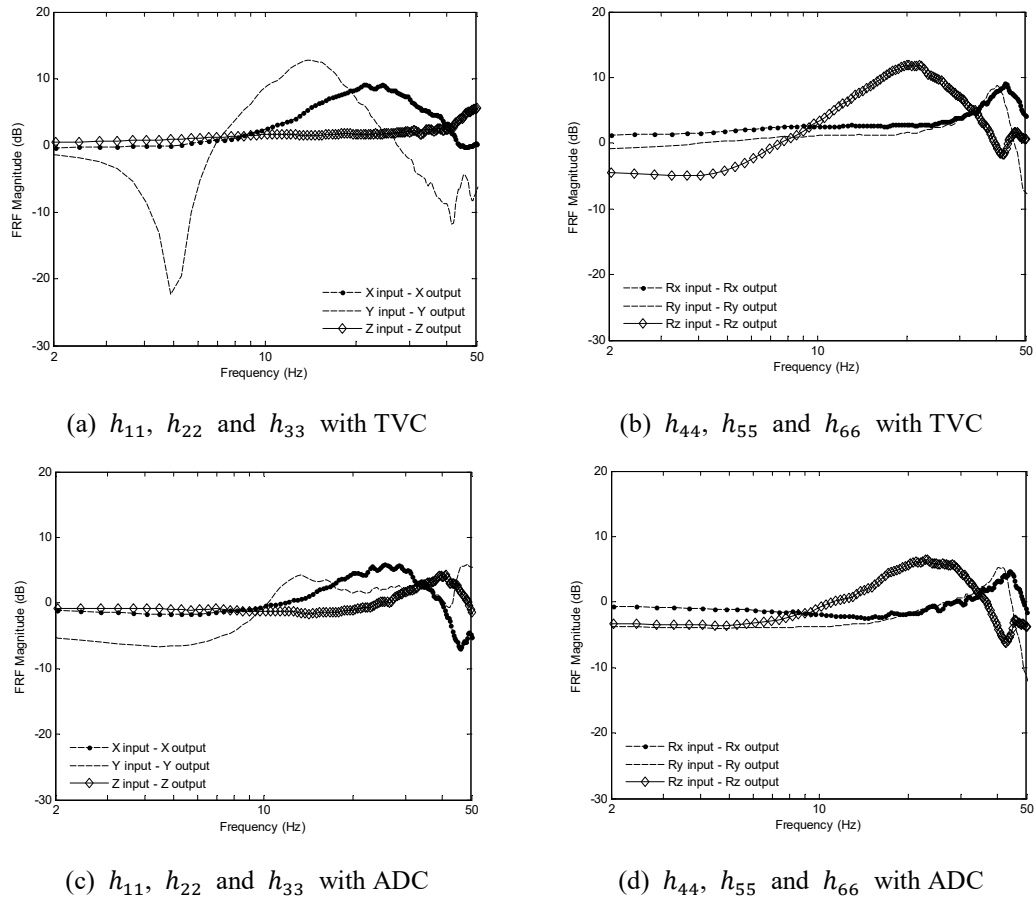

(a) h_{11}, h_{22} and h_{33} with TVC

(b) h_{44}, h_{55} and h_{66} with TVC

(c) h_{11}, h_{22} and h_{33} with ADC

(d) h_{44}, h_{55} and h_{66} with ADC

Fig. 8   Acceleration amplitude frequency response characteristics of the diagonal elements in the FRF matrix

(a) h_{51} $(rad/s^2)/g$

(b) h_{15} $g/(rad/s^2)$

(c) h_{52} (rad/s²)/g

(d) h_{25} g/(rad/s²)

(e) h_{53} (rad/s²)/g

(f) h_{35} g/(rad/s²)

(g) h_{54}
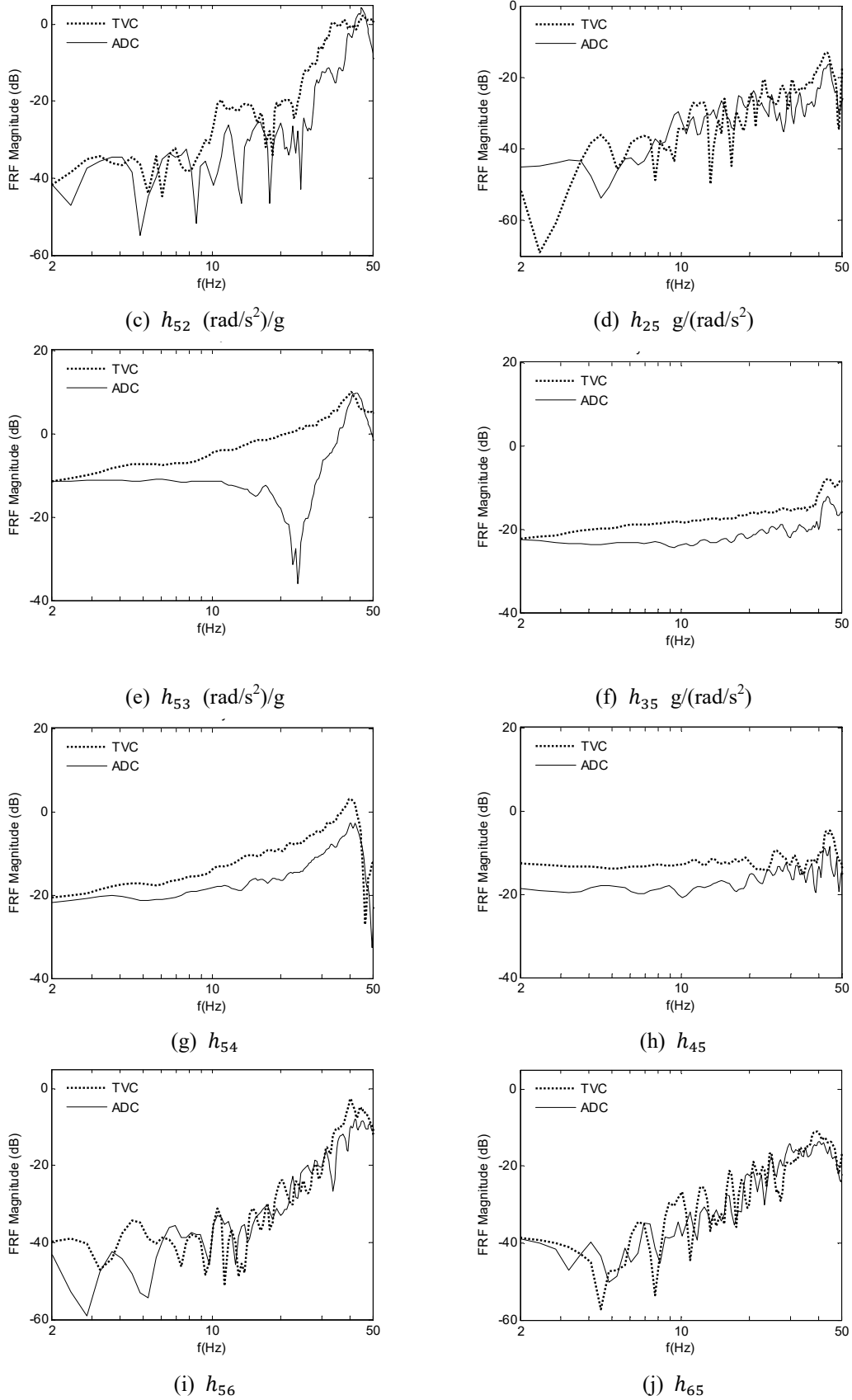
(h) h_{45}

(i) h_{56}

(j) h_{65}
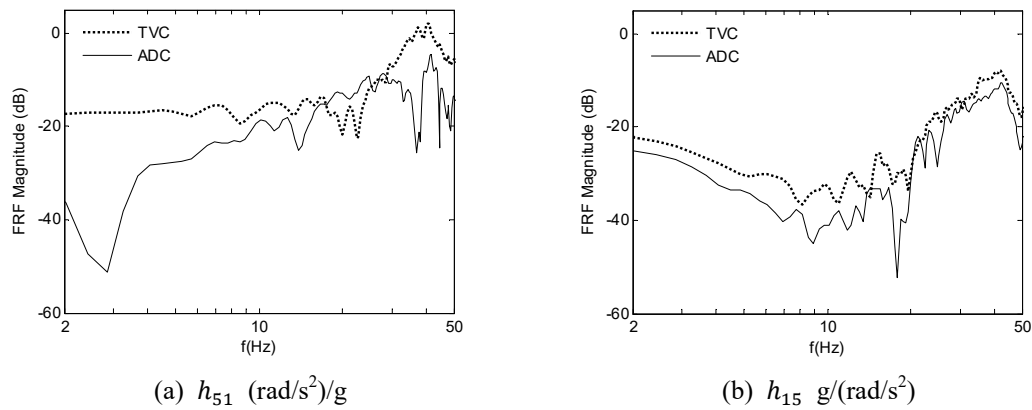
Fig. 9   Off diagonal Ry-related acceleration amplitude frequency response characteristics of the FRF matrix

Fig.8 shows that both the TVC and the ADC have a bandwidth near 50Hz except for h_{22} with TVC. A resonant frequency near 5Hz is shown in h_{22} with TVC while h_{22} with ADC shows no obvious resonant frequency.

Fig. 9 shows the cross-coupling between Ry and the other DOF. The amplitude frequency response characteristics of h_{25}, h_{56} and h_{65}, which are far less 0 dB in most frequency bands, are very similar for the two controllers. The amplitude frequency response characteristics of $h_{51}, h_{52}, h_{53},$ h_{54}, h_{15}, h_{35}, h_{45} show that the cross-couplings between Ry and other DOF are significantly reduced with ADC in most frequency bands. The best improvement with ADC is more than 30dB near 23Hz in h_{53}.

V. Conclusion

Acceleration decoupling control of 6 DOF electro-hydraulic shaking table was developed based on a modal decoupling control approach. The gravity and coriolis/centripetal forces were compensated in joint space. The control axes of the shaking table were decoupled in task space when the differences of the dynamics were cancelled and the same proportional gains were set for each DOF in modal space. A TVC input filter was used to give command feedforward which was combined with the modal decoupling control to improve the acceleration tracking performance of the system. The number of parameters for TVC is 36 for a 6 DOF shaking table. There are only 4 control parameters for the proposed control approach. Experimental results showed that improved acceleration tracking frequency responses were obtained, and the cross-coupling between the axes was very significantly reduced with the new acceleration decoupling control.

The performance of the ADC is dependent on the modeling precision. A decoupling control with the same dynamic characteristics for each axis in task space can be achieved by the cancellation of the dynamic characteristics in modal space, but only if the model is sufficiently accurate. Some model parameter errors are inevitable, and the experimental proportional gain in modal space was constrained to ensure sufficient stability margins and hence robustness of the control system in the presence of these errors. The analysis of robustness of the ADC with parameter estimation errors remains as future work. Nevertheless, the method provides a much more systematic approach to shaking table control compared to the conventional manually-tuned TVC, offering a significant improvement in seismic testing accuracy and hence earthquake safety in the future.

Funding

References

1   Tagawa Y and Kajiwara K (2007) Controller development for the E-Defense shaking table. In: Proceedings of IMechE, Part I: Journal of Systems and Control Engineering. 221: 171-181.

2   Clark AJ (1992) Dynamic characteristics of large multiple degree of freedom shaking tables. In: Proceedings of Earthquake Engineering, 10th World Conference, Rotterdam, The Netherlands, July 19-24. pp.

2823-2828.

3   Kusner DA, Rood JD and Burton GW (1992) Signal reproduction fidelity of servo hydraulic testing equipment. In: Proceedings of Earthquake Engineering, 10th World Conference, Rotterdam, the Netherlands, July 19-24. pp. 2683-2688.

4   Luco JE, Ozcelik O and Conte JP (2010) Acceleration Tracking Performance of the UCSD-NEES Shake Table. Journal of Structural Engineering, 136(5): 481-490.

5   Dozono Y, Horiuchi T, Katsumata H, et al. (2004) Shaking-table control by real-time compensation of the reaction force caused by a nonlinear specimen, Transactions of the ASME, 126: 122-127.

6   Codourey A (1998) Dynamic modeling of parallel robots for computed-torque control implementation. The International Journal of Robotics Research, 17(12): 1325-1336.

7   Yang C, Huang Q, Han J (2012). Computed force and velocity control for spatial multi-DOF electro-hydraulic parallel manipulator. Mechatronics, 22(6): 715-722.

8   Dasgupta B, Mruthyunjaya T S (1998) A Newton-Euler formulation for the inverse dynamics of the Stewart platform manipulator. Mechanism and machine theory, 33(8): 1135-1152.

9   Koekebakker SH (2001) Model based control of a flight simulator motion system. Phd thesis, Delft University of Technology, Netherlands.

10 Plummer AR (2007a) Control techniques for structural testing : a review. In: Proceedings of IMechE, Part I: Journal of Systems and Control Engineering, 221(2): 139-169.

11 Soderling S, Sharp M and Leser C (1999) Servo controller compensation methods selection of the correct technique for test applications. SAE Technical Paper 1999-01-3000.

12 Stoten DP and Shimizu N (2007) The feedforward minimal control synthesis algorithm and its application to the control of shaking-tables. In: Proceedings of IMechE Part I: Journal of Systems and Control Engineering, 221(3): 423-444.

13 Guan G F, Xiong W, Wang H T (2016) Adaptive random control of a two-axis redundantly actuated electro-hydraulic shaking table. Journal of Vibration and Control, 22(16): 3455-3469.

14 Gang S, Zhen-Cai Z, Lei Z, et al. (2013) Adaptive feed-forward compensation for hybrid control with acceleration time waveform replication on electro-hydraulic shaking table. Control engineering practice, 21(8): 1128-1142.

15 Plummer A R. (2004) Modal control for a class of multi-axis vibration table. UKACC Control 2004 Mini Symposia. UK, pp. 111-115.

16 Plummer A R, Guinzio P S (2009) Modal control of an electrohydrostatic flight simulator motion system. ASME 2009 Dynamic Systems and Control Conference. American Society of Mechanical Engineers, pp. 345-352.

17 Jiang H Z, He J F, Tong Z Z (2012) Modal space control for a hydraulically driven Stewart platform. Journal of Control Engineering and Technology, 2(3): 106-115.

18 He J, Jiang H, Tong Z (2017) Modal control of a hydraulically driven redundant actuated fully parallel mechanism. Journal of Vibration and Control, 23(10): 1585-1592.

19 Plummer A R (2016) Model-based motion control for multi-axis servohydraulic shaking tables. Control Engineering Practice, 53: 109-122.

20 Merlet J P (2006) Parallel robots. Springer Science & Business Media.

21 Plummer AR (2007) A general co-ordinate transformation framework for multi-axis motion control with applications in the testing industry. Control Engineering Practice, 18(6): 598-607.

22 Underwood M A, Keller T (2006) Applying coordinate transformations to multi-DOF shaker control. Sound and Vibration, 40(1): 14-27.

23   Jelali M, Kroll A (2012) Hydraulic servo-systems: modelling, identification and control. Springer Science & Business Media.

24   Iwasaki M, Ito K, Kawafuku M, et al. (2005) Disturbance observer-based practical control of shaking tables with nonlinear specimen. Proc. of the 16th IFAC World Congress on Automatic Control.

25   Horiuchi, T., & Konno, T. (2001). Shaking Table and Method of Controlling The Same. U.S. Patent No. 6189385. Washington, DC: U.S. Patent and Trademark Office.

26   The MathWorks Inc (2003) xPC Target User's Guide, version 2.0.2. Available at: http://www.mathworks.com/support/product/XP/productnews.

27   Zhang SY, Han JW and Zhao H (2004) RCP and RT Control of 6-DOF Parallel Robot, In Fourth International Workshop on Robot Motion and Control, Finland, pp. 133-137.